American Mineralogist, Volume 78, pages 794–803, 1993

CO_2 contents and formation pressures of some Kilauean melt inclusions

ALFRED T. ANDERSON, JR., GEORGIA GILLILAND BROWN
Department of the Geophysical Sciences, The University of Chicago, 5734 S. Ellis Avenue, Chicago, Illinois 60637, U.S.A.

ABSTRACT

Of 50 analyzed glass inclusions in olivine phenocrysts from the 1959 Kilauea Iki eruption, 41 formed at pressures <1 kbar, seven between 1 and 2 kbar, and two at pressures >2 kbar. The surprisingly low formation pressures suggest that most 1959 olivines, including most of those with preeruptive equilibration temperatures above 1200 °C, crystallized in an upper part of Kilauea's summit magma storage reservoir. The implication that the parental magma was buoyant relative to stored magma is consistent with an expected preeruptive bulk CO_2 content near 0.2 wt% and published evidence for mixing between hot, newly arrived parental and preexisting magma. That the 1959 magma was rich not only in crystals but also in gas, as evidenced by its high lava fountains, suggests that the storage time in a shallow reservoir was too short for either crystals or gas to be lost. Therefore, the 1959 Kilauean magma probably is a near-parental magma that rose and formed a gas- and crystal-rich cap near the top of a shallow body of stored magma beneath Kilauea's summit region. Whether newly arriving parental magma is buoyant relative to stored magma depends mainly on pressure and magma gas content. Consequently, it seems likely that the eruptive and degassing behavior of Kilauea is regulated in part by an interplay between the CO_2 content of parental magma and the pressure at which new magma intrudes stored, degassed magma.

BACKGROUND ON THE 1959 ERUPTION OF KILAUEA

Kilauea is an evolving as well as active volcano. An explosive eruption in 1924 marked the end of a long period of nearly continuous summit lava lake activity and probably recorded extensive draining of a magma storage reservoir (perhaps by erupting into deep sea water along the submarine East Rift; Holcomb et al., 1988) that allowed ground water to enter and power the explosions. After an unusually long interval of inactivity, eruptions resumed in 1952, and important summit and flank eruptions occurred in 1954 and 1955, respectively. Geodetic (Fiske and Kinoshita, 1969) and geochemical studies (Wright et al., 1975) of activity during the 1960s revealed the evolving summit magma storage reservoir to consist of separate inflation centers occupied by compositionally distinct magma batches. It seems likely that the summit magma storage reservoir consisted of separate magma compartments in 1959 also, but it evolved into a more continuous body with gradational compositional transitions during the 1980s (Helz, personal communication; Thurber, 1987; Ryan, 1987a, 1987b).

The 1959 eruption of Kilauea (the Kilauea Iki eruption) occurred near the summit of Kilauea at the edge of Kilauea caldera. It produced the highest fire fountains (up to about 400 m) observed at Kilauea up to that time (Richter et al., 1970). The erupted basalt varied in composition and olivine content (much of it contained about 20 wt% of olivine) and is appropriately termed a tholeiitic picrite. In general, eruptive temperature, fountain height, olivine content, and glass MgO content correlated positively during the eruption (Murata and Richter, 1966). A deep swarm of seismicity occurred 3 months before the eruption in mid-August and suggests that magma began to rise from mantle depths of 45–60 km at that time (Eaton and Murata, 1960; Eaton, 1962). The precursory seismic and geodetic signals indicate that new magma entered the summit magma reservoir at a high rate for a period of 6 weeks or less prior to the onset of the eruption (Eaton et al., 1987). Drainback occurred after most eruptive episodes, that is, some lava from the surface lava lake drained back into the vent, thereby bringing cooler surficial material into contact with magma below (Richter et al., 1970; Eaton et al., 1987).

Compositional and textural studies by Helz (1987) and Schwindinger (1987) confirm the earlier work of Wright (1973) in revealing that the 1959 magmas resulted from the mixing of compositionally distinct magmas. Rounded augite phenocrysts in early-erupted lava (Murata and Richter, 1966) and glass compositions (Schwindinger, 1987) suggest that one of the magmas evolved by dissolving augite and crystallizing olivine.

Several textural varieties of olivine occur in the 1959 scoria (Helz, 1987; Schwindinger and Anderson, 1989): (1) crystals (some with kink bands of deformation origin) with mostly round edges and corners; (2) euhedral crystals, a few of which are skeletal or amoeboid; (3) rare other textural types. The crystals are variously zoned, and those in the first group are commonly reversely zoned with Mg-rich rims. Many of the euhedral crystals are also

0003–004X/93/0708–0794$02.00

reversely zoned. The reverse zoning is most prevalent in early-erupted phases, and most late erupted olivines are normally zoned (Helz, 1987; Schwindinger, 1987). Schwindinger and Anderson (1989) concluded that zoning developed mostly in a matter of days, but some large, weakly zoned crystals possibly reflect zoning that developed over approximately a month.

Glass surrounding olivines varies in composition and is notably poor in Mg around some rounded crystals that appear to have been partially resorbed (Helz, 1987). Helz (1987, p. 714–715) suggested: "Olivine crystals from a cooler part of the magma chamber were swept up in hotter, more mobile liquid. A thin layer of less magnesian, cooler, and hence slightly more viscous liquid moved with the crystals. . . . The melt began to resorb the adjacent olivine. . . ."

Helz (1987) considered that the geophysical and petrological observations could be best explained if the hotter of two magmatic components were "liberated during the August earthquake swarm and reached the base of the shallow reservoir in late September. . . . the magma followed a seldom-used path . . . encountering an older batch of stored magma. It broke through this older chamber bringing some of the stored magma with it." Evidently a range of liquids and crystals mixed together for some days or weeks before being coerupted. It is plausible that mixing occurred during the 6 week preeruptive period of rapid summit inflation.

Samples of basaltic scoria were collected approximately daily during the 1959 eruption by U.S. Geological Survey personnel from the Hawaiian Volcano Observatory at a location about 1 km south of the fire fountain. Portions of these samples were kindly made available to us for study by Thomas L. Wright. A.T.A. collected some additional material in 1986 from the walls of a collapse pit near the caldera rim southwest of Byron's Ledge, near the original sample locality. The latter samples (numbered according to depth in centimeters below the 1986 surface—some wind erosion probable) were collected at successive levels downward from the ground surface to a total depth of 220 cm. Isopach maps of the 1959 tephra fall deposit (Richter et al., 1970) suggest that the total thickness of 1959 tephra at this point is $<\sim 3$ m. Scoria at 220 cm is unlike material erupted during most of the first eruptive episode. Some of the overlying horizons are olivine-rich and probably correspond to the olivine-rich material erupted during some December eruptive phases. Deposition of scoria was episodic southwest of the vent and included a heavy fall of olivine-poor scoria during the November 28–29 eruptive episode (Richter et al., 1970). Although the eruptive stages of Anderson's 1986 collapse pit samples are not yet established, scoria above 220 cm probably were deposited after the first eruptive phase ended on November 21, 1959.

Fourteen of our 50 analyses are of inclusions in olivines from field sample Iki 22, which was erupted on November 18 during the first eruptive phase, before significant drainback, and which was one of the hottest, most olivine-rich magmas. This sample contains the most MgO-rich glass and is rich in the CaO-rich S1 end-member (68% S1 end-member according to Wright, 1973) that Helz (1987) associated with the newly arrived, high-temperature end-member. As magma that erupted during the first eruptive phase formed more than half of the lava lake (Richter et al., 1970), our 18 inclusions that were erupted during the first phase (including four from Iki 5, which was collected on the last day of the first eruptive phase) are roughly proportional to the amount of lava erupted during that phase.

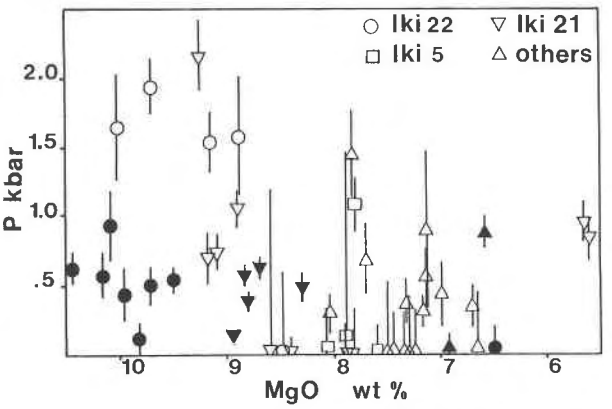

Fig. 1. Pressures at which melt inclusions from Kilauea's 1959 eruption would be saturated with a $CO_2 + H_2O$ gas. All inclusions are in olivine host crystals. MgO decreases to the right so that the sample groups are mostly in eruptive sequence. Solid symbols designate inclusions that lack gas bubbles. Open symbols correspond to pressures for bubble-bearing inclusions after restoring their bulk CO_2 concentrations for a 0.5 vol% gas bubble in equilibrium with melt at 1200 °C. Uncertainty in MgO is about 0.1 wt%, absolute. Error limits for pressures are explained in Table 1, footnotes F–H. Three inclusions not analyzed for MgO are plotted at arbitrary MgO values (see Table 1). Inclusion Iki 22-8 has a saturation pressure of 5.1 kbar and is not plotted.

Results and discussion

We present new observations of textural features and electron microprobe and infrared spectroscopic analyses of glass inclusions and their host olivine phenocrysts (Table 1, Fig. 1).

Textures

Two kinds of glass inclusions are present in the Kilauea Iki olivines: inclusions with gas bubbles and inclusions without bubbles. Observed bubble sizes are polymodal: 15 inclusions have no bubbles, 16 inclusions have 2.1–3.0 vol% bubbles, and six inclusions have 4.1–7.0 vol% bubbles (Table 1). Inclusions in individual olivine crystals have similar bubbles: in some crystals all melt inclusions, regardless of size, lack bubbles; in other crystals from the same centimeter-sized scoria clast most or all inclusions may have bubbles (Fig. 2). Such a distinctive organization of bubble-bearing and bubble-free inclusions could hardly result from random or volume-depen-

TABLE 1. Textures and compositions[A] of melt inclusions and host olivines

Sample[B]	22-1-11	22-8	22-2 (1)	22-4B1	22-4B2	22-12E	22-13A	22-13B	22-13C 1	22-13C 2
SiO_2	49.37	50.29	48.84	51.04	49.98	48.16	48.44	49.15	48.91	49.19
Al_2O_3	11.79	12.09	12.20	11.55	12.14	12.04	12.30	12.00	12.60	11.54
FeO[C]	12.37	11.83	12.23	11.97	11.94	13.11	12.65	12.84	11.99	12.21
MgO	9.15	8.50	10.16	9.95	9.82	9.71	8.88	10.02	10.43	10.08
CaO	12.19	11.69	10.97	11.30	11.78	11.56	12.37	10.69	10.45	11.46
Na_2O	1.98	1.90	2.09	1.99	2.09	2.06	1.90	2.03	2.23	1.96
K_2O	0.36	0.50	0.51	0.17	0.21	0.46	0.48	0.50	0.48	0.51
TiO_2	2.40	2.80	2.58	1.81	1.89	2.40	2.55	2.36	2.47	2.65
P_2O_5	0.25	0.27	0.27	0.10	0.15	0.41	0.28	0.27	0.33	0.26
S	0.14	0.13	0.15	0.12	0.00	0.09	0.15	0.14	0.11	0.14
Sum[D]	95.68	97.08	96.46	99.21	99.41	96.10	97.28	98.05	101.01	96.68
H_2O[E]	0.63	0.70	0.60	0.62	0.95	0.73	0.76	0.71	0.60	0.63
CO_2[F] (ppm)	223 ± 35	758 ± 48	210 ± 64	157 ± 75	0 ± 50	174 ± 48	227 ± 65	239 ± 58	229 ± 41	349 ± 93
P (bars)[G]	605 ± 90	2070 ± 137	567 ± 163	436 ± 190	110 ± 124	498 ± 122	639 ± 94	660 ± 150	616 ± 106	933 ± 246
P_t[H]	1526 ± 232	5087 ± 315					1580 ± 434	1650 ± 387		
Ol (Fo)[I]	no data	87.8 u	85.9 r	87.1 nd	87.0 u	86.7 nd	87.3 nd	86.5 nd	86.8 nd	86.8 nd
Ol size[J]	1190	1014	324	735	970	882	672	1378	758	523
Incl. D.[K]	209	145	99	98	97	150	110	149	180	181
Shape[L]	round	round	round	round	round	faceted	round	round	round	round
Bubbles[M]	1	1	0	0	0	0	1	1	0	0
Gas vol%[N]	2.6	2.2	0	0	0	0	2.2	3.7	0	0
Chrom.[O]	several	several	few	few	many	several	several	several	several	several
Gas incl.[P]	no data	no data	no data	no	no	yes	no	no	no	no
T[Q]	1198	1185	1218	1214	1211	1209	1192	1215	1225	1217

Sample[B]	22-12B	22-1-9	22-1-10	22-4	5-9	5-11a	5-12	5-14	220-I3	220-4-1
SiO_2	49.62	51.24				49.70		49.91	52.34	51.69
Al_2O_3	12.13	14.13				12.74		13.07	14.57	12.95
FeO[C]	12.49	10.49				11.76		11.44	8.28	10.58
MgO	8.47	6.50	9.5	9.7	7.6	7.89	7.80	8.07	7.13	7.32
CaO	11.87	11.47				12.14		11.49	10.92	11.68
Na_2O	1.93	2.68				2.08		2.30	2.77	2.11
K_2O	0.43	0.51	0.35	0.48	0.44	0.51	0.53	0.54	0.62	0.53
TiO_2	2.66	2.60	2.12	2.42	2.82	2.71	2.66	2.73	2.83	2.77
P_2O_5	0.23	0.33	0.19	0.24	0.27	0.30	0.26	0.30	0.40	0.27
S	0.17	0.05	0.07	0.14	0.03	0.17	0.13	0.15	0.14	0.10
Sum[D]	97.96	97.28				94.97		98.63	92.66	98.77
H_2O[E]	0.44	0.66	0.66	0.66	0.55	1.12	0.84	0.77	0.48	0.63
CO_2[F] (ppm)	0 ± 91	0 ± 84	197 ± 30	286 ± 30	0 ± 30	0 ± 196	150 ± 30	0 ± 42	132 ± 85	51 ± 24
P (bars)[G]	24 ± 223	54 ± 206	544 ± 77	772 ± 78	37 ± 74	153 ± 492	459 ± 76	73 ± 103	353 ± 212	174 ± 59
P_t[H]	24 ± 597			1950 ± 198	37 ± 197	153 ± 1322	1085 ± 201	73 ± 278	897 ± 563	385 ± 158
Ol (Fo)[I]	87.0 u	87.5 r	86.4 r	88.0 u	87.0 n	no data	87.2 r	87.2 r	87.4 nd	86.4 r
Ol size[J]	517	1615				1305	539	539	990	1395
Incl. D.[K]	94	160				69	126	126	110	279
Shape[L]	faceted	faceted				round	round	round	round	faceted
Bubbles[M]	1	0	0	1	1	1	1	1	1	1
Gas vol%[N]	0.3	0	0	3.0	11.0	2.3	2.7	2.7	5.4	1.5
Chrom.[O]	few	few				few	few	few	few	few
Gas incl.[P]	no	no				no	no	no	no	yes
T[Q]	1184	1145	1205	1209	1167	1173	1171	1176	1157	1161

[A] Compositions are in weight percent unless otherwise noted. Analyses were performed using the University of Chicago electron microprobe with help from Ian Steele and Fangqiong Lu. Microprobe standards were simple oxide crystals and glasses, together with apatite (P_2O_5) and troilite (FeS for S). A combination of crystal-focusing and energy-dispersive methods was used as detailed in Schwindinger (1987). The rows above that for Sum record values that are normalized to 100%. Inclusion 22-4B2 has unexplained low S. MgO values in parentheses are arbitrary values used for plotting purposes on Fig. 1.

[B] Sample numbers refer to the following materials: all samples beginning with 22, 5, and 21 are from the Iki 22, Iki 5, and Iki 21 scoria samples erupted and collected on November 18, 21, and December 11, 1959, respectively. Other numbers such as 220, 45, etc., refer to the distance in centimeters below the surface about 1 km south of the vent where scoria were collected by A.T. Anderson in 1986. The sample numbers correspond to entries in our laboratory notebooks and have variable significance with regard to scoria clast number, aggregate number, crystal number, and inclusion number. The following groups of inclusions are from either the same aggregate or the same crystal: 22-4-B1 and B2, 22-13-C1 and C2, 58-1-1 and 2, 58-3-1 and 2, 45-C1 and C2, 45-A1 and A2, 45-B and B2, 21-1A-A and B, 21-1B-A and B, 21-1C-A and B, 21-2A-A and B, 21-2B-A and B. The sample groups are presented in probable eruptive sequence.

[C] Fe_{tot} as FeO.

[D] The original microprobe sum of all entries in rows above Sum. Some low sums reflect various difficulties related to manipulation of fragile, doubly polished crystals: some were poorly polished; to allow removal after analysis, some were mounted in an acetone-soluble plastic that deformed under vacuum; some analysis conditions were optimized for analysis of olivine, not glass. In general the recorded concentrations are considered accurate within 2–5% of the amount reported.

[E] The weight percent of H_2O_{tot} (OH^- + H_2O molecular) as H_2O as determined spectroscopically from the height of the absorption peak at about 3535/cm using pinholes 40–100 μm in diameter to mask the inclusions in the microbeam chamber of a Nicolet 60SX FTIR spectrometer. A MCTA detector and KBr beam splitter were used because the principal emphasis was on CO_2. Concentrations were calculated using the Beer-Lambert law and assuming a molar absorption coefficient of 63 L/(mol·cm) from Dobson and others cited in Dixon et al. (1988). The room temperature density of all basaltic glasses was taken to be 2.8 g/cm^3. Glass thicknesses were measured by viewing the crystals edgewise in immersion oils under a

TABLE 1.—*Continued*

Sample[B]	220-1	160A-I2	58-1-1	58-1-2	58-2-1	58-3-1	58-3-2	45-C1	45-C2	45-6-1
SiO_2	51.83	50.64	51.68	51.96	51.85	51.48	50.60	51.00		52.34
Al_2O_3	13.88	12.51	13.18	12.88	13.52	13.78	14.05	13.98		13.28
FeO[C]	7.85	11.05	9.94	10.04	8.92	9.08	9.56	8.48		8.78
MgO	8.06	7.67	6.58	6.69	7.16	7.24	6.98	7.56	(7.4)	6.65
CaO	12.14	12.07	12.42	12.32	12.67	12.17	12.37	13.10		13.08
Na_2O	2.53	2.28	2.23	2.08	2.19	2.29	2.35	2.39		2.07
K_2O	0.52	0.54	0.55	0.60	0.59	0.64	0.57	0.53		0.54
TiO_2	2.72	2.75	2.96	2.95	2.74	2.87	3.10	2.59		2.84
P_2O_5	0.32	0.27	0.31	0.32	0.25	0.29	0.33	0.24		0.29
S	0.15	0.18	0.15	0.16	0.11	0.16	0.09	0.13		0.13
Sum[D]	101.11	96.65	99.49	98.72	100.34	98.54	96.97	97.03		99.40
H_2O[E]	0.72	0.69	0.24	0.27	0.41	0.39	0.32	0.43	0.35	0.63
CO_2[F] (ppm)	34 ± 20	94 ± 38	346 ± 40	53 ± 23	45 ± 17	0 ± 49	66 ± 36	0 ± 76	0 ± 45	0 ± 67
P (bars)[G]	147 ± 49	290 ± 94	880 ± 106	138 ± 56	130 ± 42	19 ± 119	174 ± 89	23 ± 186	15 ± 110	49 ± 164
P_r[H]	289 ± 132	680 ± 252		355 ± 151	315 ± 112	19 ± 320	444 ± 236	23 ± 498	15 ± 294	49 ± 442
Ol (Fo)[I]	86.9 n	87.4 u	87.4 r	no data	86.8 n	87.4 r	no data	86.9 nd	86.8 u	86.3 r
Ol size[J]	793	783	481	529	1125	1684	1684	1344	702	1060
Incl. D.[K]	168	174	154	154	252	273	241	84	156	212
Shape[L]	faceted	round	round	round	round	round	faceted	round	round	round
Bubbles[M]	1	1	0	1	1	1	1	1	1	1
Gas vol%[N]	5.1	2.1	0	3.2	3.0	2.3	2.3	2.7	5.5	5.0
Chrom.[O]	few	several	several	several	several	many	many	few	many	several
Gas incl.[P]	no	no	no	no	no	no	no	no	yes	no
T[Q]	1176	1168	1146	1148	1158	1159	1154	1166		1148

Sample[B]	45-A1	45-A2	45-B	45-B2	25-5-1	21-1A-A	21-1A-B	21-1B-A	21-1B-B	21-1C-A
SiO_2	50.34	51.60	50.84	51.14	52.75	51.81		49.82	50.88	50.98
Al_2O_3	14.16	14.06	13.41	14.18	13.20	14.28		12.09	12.26	12.77
FeO[C]	8.28	8.30	8.84	8.35	8.24	10.30		13.38	13.08	10.55
MgO	7.83	6.92	7.35	7.32	7.13	5.60	(5.65)	8.83	8.68	9.16
CaO	12.99	13.02	12.86	12.31	12.74	11.77		10.60	10.67	11.23
Na_2O	2.60	2.35	2.38	2.75	2.19	2.48		2.04	2.04	2.19
K_2O	0.41	0.51	0.63	0.62	0.54	0.57		0.47	0.42	0.40
TiO_2	2.85	2.81	3.16	2.85	2.79	2.76		2.39	2.22	2.38
P_2O_5	0.39	0.28	0.35	0.32	0.30	0.30		0.21	0.26	0.24
S	0.15	0.15	0.18	0.17	0.12	0.13		0.17	0.19	0.10
Sum[D]	99.81	97.37	97.05	95.94	99.81	96.63		97.57	97.31	97.41
H_2O[E]	0.57	0.73	0.46	0.35	0.96	0.31	0.36	0.36	0.36	0.31
CO_2[F] (ppm)	212 ± 47	0 ± 38	0 ± 52	0 ± 60	67 ± 30	125 ± 23	144 ± 21	222 ± 28	247 ± 27	104 ± 28
P (bars)[G]	568 ± 120	66 ± 93	26 ± 127	15 ± 146	279 ± 74	319 ± 57	371 ± 53	569 ± 72	633 ± 68	267 ± 70
P_r[H]	1443 ± 312		26 ± 341	15 ± 392	562 ± 201	831 ± 152	962 ± 139	—	—	692 ± 186
Ol (Fo)[I]	88.8 u	88.3 u	88.3 u	88.1 u	87.3 n	86.3 n	86.4 n	84.0 u	83.9 u	87.3 u
Ol size[J]	902	664	706	706	891	943	943	2068	2068	2122
Incl. D.[K]	124	143	121	79	198	253	175	375	263	328
Shape[L]	round	round	round	round	round	round	round	faceted	faceted	round
Bubbles[M]	1	0	1	1	1	1	1	0	0	1
Gas vol%[N]	6.9	0	3.4	6.6	2.5	2.9	2.2	0	0	1.9
Chrom.[O]	several	several	several	several	few	several	several	few	few	many
Gas incl.[P]	no	no	no	no	no	no	no	no	no	no
T[Q]	1171	1153	1162	1161	1157	1127		1191	1188	1198

petrographic microscope and using an ocular with a calibrated reticle. Although uncertainties in H_2O_{tot} vary from one inclusion to another, all are <10% of the amount reported.

[F] The concentration of C in the glass is reported as parts per million (by weight) of CO_2. The concentrations are based on visually smoothed infrared absorption peak heights at about 1515/cm and 1435/cm caused by CO_3^{-2} in the glass. The molar absorption coefficient was taken to be 375 L/(mol·cm) (Fine and Stolper, 1986). The instrumental configuration, glass density, and thicknesses were as given in footnote E. Following Dixon (personal communication) most spectra were read after subtracting a spectrum of outgassed lava lake glass (<10 ppm of CO_2) such that the difference spectrum has a constant average background in the spectral region of interest. In some cases unsubtracted (raw) spectra were read because the subtracted spectra contained some apparent artifacts. Errors include contributions from thickness measurements (<5% relative uncertainty) but most are dominated by spectral noise. We have estimated the spectral errors by adding one-half the noise of the absorption peaks to one-half that of the background. Visual smoothing averages the noise; consequently, we think that our estimated errors are generous estimates of imprecision.

[G] The pressure, *P*, is that calculated at which a basaltic melt at 1200 °C and with the observed concentrations of H_2O and CO_2 remaining dissolved in the glass would be saturated with a gas. The calculations are explained in the text and are based on solubility rules from Hamilton et al. (1964) and Stolper and Holloway (1988). Errors are based on the uncertainty in the CO_2 content (footnote F).

[H] The restored pressure, P_r, is calculated as in footnote G, but is based on the bulk CO_2 content of the inclusion that is derived by adding 0.5 vol% of equilibrium gas at the indicated *T* and *P* to that remaining in the glass (footnote G). Errors are based on uncertainties regarding the amount of CO_2 in a 0.5 vol% gas bubble. See text.

[I] Host olivine composition given as mol% Fo based on 100[Mg/(Mg + Fe)] on an atomic basis. Compositions given are those observed within about 100 μm of the melt inclusions. Other symbols: u = unzoned, r = reversely zoned (rims rich in Fo), n = normally zoned, nd = not determined.

[J] Olivine size is a rough average diameter of the host olivine crystal in micrometers.

[K] Inclusion diameter is a rough average diameter of the glass inclusion, also in micrometers.

[L] The shapes of the glass inclusions. Faceted means that a major portion

TABLE 1.—*Continued*

Sample[B]	21-1C-B	21-1D-A	21-1E-A	21-2A-A	21-2A-B	21-2B-A	21-2B-B	21-2C-A	21-2D-A	21-3
SiO_2	50.40	49.69		50.32	50.20	51.76	51.29	50.39	49.55	50.03
Al_2O_3	13.06	12.47		12.60	13.05	13.36	13.18	12.91	11.58	12.56
FeO[C]	10.68	11.87		10.90	10.92	10.09	10.36	10.35	12.02	11.42
MgO	8.59	8.85	(8.3)	8.94	7.81	7.93	8.49	9.07	8.81	9.24
CaO	11.78	11.58		11.60	12.18	11.42	11.28	11.78	12.59	11.12
Na_2O	2.16	2.10		2.03	2.17	2.22	2.22	2.20	1.92	2.17
K_2O	0.43	0.46		0.54	0.51	0.37	0.39	0.41	0.51	0.54
TiO_2	2.49	2.58		2.66	2.67	2.43	2.41	2.51	2.61	2.57
P_2O_5	0.27	0.29		0.26	0.32	0.27	0.23	0.23	0.24	0.28
S	0.14	0.11		0.15	0.17	0.15	0.15	0.15	0.17	0.07
Sum[D]	97.55	98.93		97.45	98.94	98.16	98.22	98.47	96.13	97.45
H_2O[E]	0.50	0.38	0.38	0.31	0.31	0.31	0.25	0.35	0.35	0.58
CO_2[F] (ppm)	0 ± 176	157 ± 20	187 ± 38	51 ± 19	0 ± 53	0 ± 32	0 ± 19	110 ± 19	153 ± 26	320 ± 38
P (bars)[G]	31 ± 436	405 ± 50	481 ± 96	136 ± 46	12 ± 129	12 ± 78	8 ± 35	285 ± 47	393 ± 66	848 ± 100
P_r[H]	31 ± 1161	1050 ± 132	—	—	12 ± 346	12 ± 208	8 ± 123	736 ± 125	—	2160 ± 252
Ol (Fo)[I]	87.9 u	87.1 u		85.9 u	86.7 u	87.8 r	87.5 r	88.7 u	86.1 u	85.8 n
Ol size[J]	1077	1176	1387	865	865	1079	1079	1060	1051	2901
Incl. D.[K]	190	428	267	320	134	192	150	228	262	379
Shape[L]	round	round	faceted	round	round	round	round	round	round	round
Bubbles[M]	1	9	0	0	1	1	1	1	0	2
Gas vol%[N]	1.7	1.3	0	0	1.0	1.6	1.7	1.0	0	2.1
Chrom.[O]	many	several	several	few	few	many	many	few	many	several
Gas incl.[P]	no	no	no	no	no	yes	yes	no	no	no
T[Q]	1187	1192		1194	1171	1173	1185	1196	1191	1200

of the total surface contact between glass and host olivine consists of flat crystal faces.

[M] The number of bubbles present in the inclusion based on three dimensional observations prior to sectioning.

[N] The volume percent of gas in bubble-bearing glass inclusions. The amounts are approximate and are based on the cube of the ratio of the diameter of the bubble to that of the whole inclusion times 100.

[O] The occurrence of included crystals of chromite in the olivine phenocryst. Various olivines have more or less included chromite.

[P] Gas-rich inclusions are present in some of the olivines together with the analyzed glass inclusions. No = no gas-rich inclusions are present.

[Q] The preeruptive olivine-melt equilibration temperature, based on the wt% of MgO in the inclusion glass and the geothermometer of Helz and Thornber (1987).

dent nucleation of bubbles during cooling. Furthermore, most big as well as little inclusions contain only one bubble. If nucleation probability is volume dependent, then big inclusions should have more numerous bubbles. Our interpretation is that bubble-free inclusions lacked bubbles prior to eruptive quenching and that bubble-bearing inclusions contained preeruptive bubbles that variably expanded (commonly to about 2.5 vol%) during eruptive quenching.

Six of the seven inclusions with >9.5 wt% MgO are bubble-free. Because heating leads to melt expansion, overpressure, and inclusion rupture and because cooling causes shrinkage and bubble formation, the compelling association between high MgO (and thus high preeruption equilibration temperature) and bubble absence suggests that the bubble-free inclusions were close to or above their initial entrapment temperatures at the time of eruption.

Most of the inclusions, including most of the bubble-free inclusions (Fig. 3), are similar to Wright's (1973) CaO-rich parental magma that Helz (1987) concluded to be of deeper, newer, and hotter derivation. The large range in CaO contents of the inclusions suggests that they formed during magma mixing. Significant changes in inclusion CaO due to either redistribution of CaO between olivine and inclusion (see Jurewicz and Watson, 1988) or crystallization of exceptionally Fe-rich olivine on inclusion walls are possible, but unlikely, because olivine zoning in both FeO and CaO is $<\sim 50$ and 10% (relative), respectively (Schwindinger, 1987; Anderson, unpublished data). Similar proportions of textural and zoning properties between our inclusion-bearing olivines (Table 1) and olivines described by Helz (1987), Schwindinger and Anderson (1989), and Schwindinger (1987) suggest that our inclusion-bearing olivines are broadly representative of the general population of 1959 olivine. Accordingly, we think that most of the 1959 olivine formed as cool, stored magma mixed with and cooled a fresh batch of hot parental magma, high in CaO, that was derived from a deep source.

The evolution of host melt compositions by means of augite solution and olivine crystallization, as suggested by Murata and Richter (1966) and Schwindinger (1987), can explain the large range in CaO concentrations in high-MgO, bubble-free inclusions. Plausibly, such augite solution and olivine crystallization occurred as hot parental magma ascended and mixed with cool stored magma during the preeruptive weeks of rapid inflation of the summit reservoir or during the eruption.

H_2O AND CO_2 CONTENTS

Our spectroscopic analyses for H_2O and CO_2 followed procedures developed by Stolper (1982), Newman et al. (1986), and Dixon et al. (1988). Some of our errors are greater than what was reported by the above workers because of limitations in analyzing melt inclusions as com-

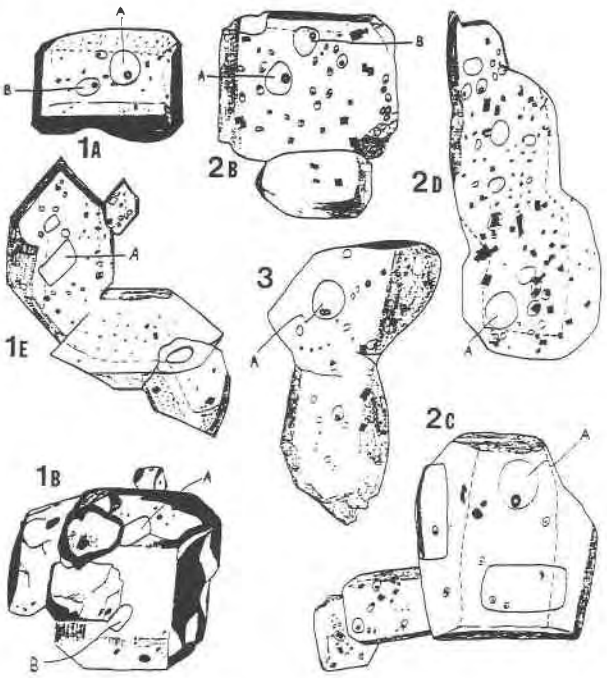

Fig. 2. Sketches of representative olivine phenocrysts from the Kilauea Iki eruption, erupted on December 11, 1959 (field sample Iki 21 = S-19 of Murata and Richter, 1966). Crystals were sketched by G.G. Brown while viewed whole and immersed in refractive index liquid under a petrographic microscope. Shading and dashed lines reveal crystal faces and edges; solid lines show outlines of melt inclusions and gas bubbles. Analyzed melt inclusions are lettered A and B. Black inclusions are chromite crystals. The abbreviated labels (for example 1A) correspond to those in Table 1 (21-1A). The aggregates vary in size and have notable features as follows: 1A (1.1 mm long), 2B (1.2 mm long; all glass inclusions have bubbles; note inclusions of gas in lower right corner of larger crystal), 2D (2.5 mm long; note most glass inclusions lack gas bubbles; some crystal edges are round), 2C (1.1-mm vertical dimension), 1B (2.3 mm long; the two inclusions are bubble-free and in the same crystal), 1E (largest crystal is 1.7 mm long; all inclusions are bubble free; and the larger inclusions are faceted; attached crystals are in parallel, perpendicular, and irrational orientations), 3 (3.9 mm long; two bubbles occur in inclusion A; and the grain boundary between the two subround crystals is almost invisible).

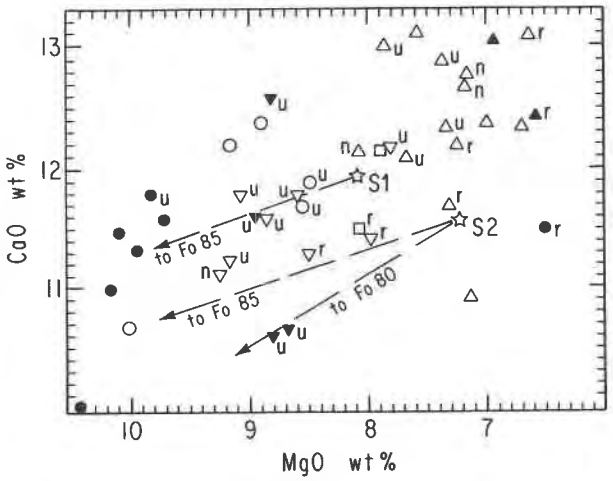

Fig. 3. Graph of weight percent CaO vs. MgO in analyzed melt inclusions (symbols as in Fig. 1; r = reversely zoned olivine host, u = unzoned, n = normally zoned). Whole rock mixing end-members S1 and S2 of Wright (1973) and Murata and Richter (1966) are plotted along with Fo 85 and Fo 80 olivine mixing lines. Helz (1987) argued that the CaO-rich member (S1) was of deeper, hotter, and more recent derivation. Uncertainties in MgO and CaO are about 0.1 and 0.2 wt%, respectively. The graph suggests that most inclusions are most closely related to the new, hot, deeply derived magma, but postentrapment compositional modifications are possible.

pared with large plates of basaltic glass where larger signals and multiple analyses are possible. As in the work of Dixon et al. (1988), we have scrutinized our spectra both with and without subtraction of reference spectra obtained from virtually CO_2-free glass from the Kilauea Iki lava lake. Errors vary from one inclusion to another (see Table 1 footnotes) and depend mostly on spectral quality; the uncertainty in sample thickness is less important.

The inclusion glasses contain 0.24–1.12 wt% H_2O and 758 to <20 ppm of CO_2 (CO_3^{-2}). Although the H_2O concentrations are mostly greater than those formerly reported for Kilauean glasses (for example, see Moore, 1965; Harris and Anderson, 1983; Dixon et al., 1991), there is much overlap. In contrast to the findings of Harris (1982 and unpublished) on submarine glasses from Kilauea and Loihi, there is no correlation between our H_2O and K_2O determinations. Lack of correlation between H_2O and K_2O is consistent with the loss or gain of volatile H_2O independent of nonvolatile K_2O. Most of our analyzed glasses with >0.60 wt% of H_2O are from hot, early-erupted material (Iki 22, November 18, 1959). Similarly, most glasses with >200 ppm of CO_2 are in early-erupted, Iki 22 olivines (because much CO_2 may reside in bubbles, this association partly reflects the preponderance of bubble-free inclusions with MgO-rich glasses). Comparatively high concentrations (and therefore pressures) of volatiles in the hot, early-erupted Iki 22 inclusions are consistent with Helz's (1987) interpretation that hot, MgO-rich melts were relatively deeply derived and minimally decompressed.

We consider that olivine is a nearly leak-free container of melt inclusions that preserves the concentrations of volatiles in the melt from which the olivine grew. Some exchange of H_2O between included and external melt may occur (e.g., Qin et al., 1992), but low C solubility (Mathez et al., 1987) and likely low diffusivity of CO_2 in olivine probably preclude significant redistribution of CO_2 on volcanological time scales. Two observations support this view: (1) inclusions in different crystals in the same aggregate may have different CO_2 contents (for example, 58-1-1 and 58-1-2, and 45-A1 and 45-A1-2), indicating that at least since becoming part of the same aggregate,

initial CO_2 concentrations have not reequilibrated; and (2) some crystals that remained above 1000 °C in the Kilauea Iki lava lake until removal by drilling in 1981 have inclusions 100 μm in diameter of CO_2 gas or liquid with densities of at least 0.3 g/cm^3 corresponding to pressures of 100 bars or greater. Such inclusions remained overpressured in CO_2 for 22 yr in the lava lake.

The CO_2 concentrations in Kilauean melt inclusions in olivine can directly reveal the approximate pressure of inclusion formation and olivine crystallization because studied Kilauean magmas are saturated with a CO_2-rich gas at pressures $> \sim 100$ bars (Roedder, 1965; Greenland et al., 1985; Gerlach and Graeber, 1985). Although some Kilauean magmas may become gas-free by degassing at low pressure and subsequently descending to greater pressures in deeper magma storage reservoirs, most of such magmas probably are cool and incapable of crystallizing much, if any, olivine.

Estimation of pressures

We present (Table 1, Fig. 1) two pressures based on our analyses: (1) a minimum pressure, P, corresponds to the concentration of CO_2 and H_2O in the glass alone; (2) for those inclusions that contain gas bubbles, we calculate a restored pressure, P_r, based on restoring an estimated amount of CO_2 in the gas bubble into a hypothetical, initially gas-free melt (negligible H_2O is in the gas bubble).

Because bubbles enlarge and decompress during quenching, we estimate their prequench size and pressure in order to assess their CO_2 content. During posteruptive quenching (a few tens of seconds) transfer of volatiles from melt to gas is negligible because the diffusivities of CO_2 and H_2O are small (Watson et al., 1982) and the inclusions are >50 μm in diameter. That many bubbles in Kilauean olivines contain a partial vacuum at room temperature (Roedder, 1965, p. 1774) is consistent with negligible exsolution of volatiles and a minimal fivefold volumetric expansion during quenching (preeruptive pressure is at least 25 bars).

We estimate that most bubble-bearing melt inclusions contained preeruptive gas bubbles amounting to 0.5 vol% of the inclusion at their eruption temperatures (1225–1145 °C, Table 1). Calculations using data and procedures summarized by Lange and Carmichael (1987) reveal that at 0.5–1.5 kbar and 1300–1100 °C the greater thermal contraction of melt compared with olivine, together with the crystallization of olivine from trapped melt, results in a 0.91 vol% gas bubble for a temperature decrease of 100 °C. Preeruptive bubble volume depends mainly on the difference between the temperature of initial formation and the equilibration temperature (plausible pressure effects are small). Temperatures of initial formation above 1300 °C are unlikely for most inclusions because bubbles in such inclusions would expand to >3 vol% and only ten of the 50 inclusions have >3 vol% gas (Table 1). Also, preeruptive cooling from 1300 to 1200 °C would decrease the pressure inside inclusions by hundreds of bars and probably cause bubble nucleation, whereas most inclusions with equilibration temperatures near 1200 °C are bubble-free. In our judgment, the prevalence of bubble-free inclusions among those with equilibration temperatures (Helz and Thornber, 1987) near 1200 °C suggests that few inclusions formed at temperatures greater than the highest equilibration temperature (1225 °C). Most equilibration temperatures exceed 1170 °C (Table 1); therefore, a reasonable total preeruptive cooling of most inclusions is <55 °C (1225–1170 °C) corresponding to a 0.5 vol% bubble. Most inclusions probably formed within the temperature interval of 1225–1170 °C and consequently cooled less. Some of the few gas-rich inclusions possibly cooled more. We assume a generous 0.5 vol% preeruptive bubble for each bubble-bearing inclusion and also consider below the effect of adding an even larger amount of CO_2 to some inclusions.

We add to each bubble-bearing inclusion the amount of CO_2 that would be in a 0.5 vol% bubble at the partial pressure of CO_2 indicated by the concentration of CO_2 in the glass (Stolper and Holloway, 1988) at a temperature of 1200 °C [used to calculate the molar volume of CO_2 in the gas as in Holloway, 1977, and Flowers, 1979; use of the equilibration temperatures would modify the resulting CO_2 concentrations and pressures by <5% (relative)]. The restored pressure, P_r, is calculated by assuming that the total estimated CO_2 content of the inclusion (dissolved in both glass and gas in the bubble) was dissolved in the melt at 1200 °C. The amount of CO_2 in the 0.5 vol% bubble increases with P because the gas is denser and richer in CO_2; P_r is commonly two to three times P (Table 1).

The total pressures include a mostly small contribution from H_2O. We used our own fitting of P_{H_2O} to H_2O solubility reported by Hamilton et al. (1964) for a Columbia River basalt. Ideality was assumed for H_2O so that the f_{H_2O} and partial pressure (P in bars) of H_2O are equal and related to concentration by

$$W = C(P)^{1/2} \tag{1}$$

or equivalently

$$P = (W/C)^2 \tag{2}$$

with $C = (0.0897 + 0.000\,006\,3)P$ (which fits the data at 1000–4000 bars of Hamilton et al., 1964, within error) where W is the wt% H_2O in the melt. The small effects of T and the basaltic melt composition on H_2O solubility were ignored. For the materials considered here, the contribution of H_2O to the gas pressure (a few tens of bars) is negligible, except for those inclusions for which the CO_2 concentration is indistinguishable from zero (with a usual error of around 30 ppm corresponding to roughly 75 bars of CO_2 pressure). In view of the minor role played by H_2O, the approximations adopted here are justified.

Most of the Kilauea Iki melt inclusions have P_r (or P for bubble-free inclusions) < 1 kbar (Fig. 1). Of the 15 bubble-free inclusions, eight formed at pressures <0.5 kbar and seven between 0.5 and 1 kbar. It is important

that most bubble-free inclusions, as well as restored bubble-bearing inclusions, have formation pressures that are dominantly <1 kbar (although some errors are large, 34 inclusions have small enough errors to make it highly probable that they formed at pressures <1 kbar).

Predominantly low formation pressures for both bubble-free and bubble-bearing inclusions are consistent with our estimate of 0.5 vol% gas bubbles in equilibrium with melt prior to eruptive quenching for most bubble-bearing inclusions. If 1 vol% of gas were assumed instead of 0.5 vol%, then restored pressures would increase by another 50–150% for inclusions with P_r = 500–1500 bars. Even with these extreme limits, it seems certain that many, if not most, of the inclusions formed and their host olivines grew at pressures <1 kbar. That surprised us.

Interpretations in the light of the 1959 eruption

The large proportion of low-pressure inclusions might have three explanations: (1) preferential survival of low-pressure inclusions; (2) formation of olivine and inclusions in a body of magma that was stored at a shallow level before active summit inflation and eruption began in 1959; (3) formation of olivine and inclusions in magma that rose to a shallow level in 1959.

Preferential survival of low-pressure inclusions upon eruptive decompression (Tait, 1992) cannot be a major factor for the Kilauea Iki inclusions because (1) most of the 1959 olivine mass is in aggregates of unbroken, faceted crystals (Schwindinger and Anderson, 1989), and (2) some gas inclusions in olivines survived up to 4 or 5 kbar of excess internal pressure during eruption (Roedder, 1965). Inclusions that cool with decompression do not become as overpressured as the isothermal case considered by Tait (1992).

In our judgment, the textures and compositions of the inclusions and their host olivine crystals are best explained if most of the olivine crystals grew and trapped inclusions during the 1959 eruption and the prior month of rapid summit inflation. We noted above that (1) the inclusions span a large range in composition (Fig. 3), which requires CaO enhancement beyond that caused by olivine crystallization, and (2) most inclusion compositions are CaO-rich like the new, hot, deeply derived magma discussed by Helz (1987). Nineteen of the 50 inclusions have compositions that are within error for a mixture of a CaO-rich melt like the S1 member of Wright (1973) and Fo 85 olivine (Fig. 3). The range in CaO displayed by inclusions in the early-erupted Iki 22 olivine crystals suggests formation from magmas that crystallized olivine either during augite reaction or during magma mixing after augite reaction rather than from two separate magmas that mixed only after olivine crystallized. Mixing and augite reaction prior to 1959 cannot be excluded, but the 1959 magmas have new compositions unlike those erupted earlier (Wright and Fiske, 1971). Helz (1987) emphasized that the high-MgO glasses, high eruption temperatures, and other unique features of the 1959 eruption pointed to the introduction of new CaO-rich magma from great depth late in 1959. Most inclusions are compositionally most similar to this CaO-rich magma. In view of the above observations, we think that the CaO-rich inclusions and their host olivines formed during the 1959 history of summit inflation and eruption.

Previous workers (Murata and Richter, 1966; Wright, 1973; Helz, 1987; Mangan, 1990) thought that various amounts of olivine in the 1959 scoria were derived from preexisting, olivine-containing bodies of magma. We agree that some of the most olivine-rich scoria probably have a large mass fraction of olivine crystals that crystallized and accumulated before summit inflation and eruption in 1959. Some reversely zoned olivines have inclusions with compositions similar to the CaO-poor (S2) end-member magma of Wright (1973). Also a significant mass fraction of olivine occurs as rare but large crystals with kink bands of deformational origin that are not likely to have formed while free swimming in melt. Various sources of olivine crystals are indicated by their varied textures (Helz, 1987; Schwindinger and Anderson, 1989), but we think that most of the inclusions formed in crystals that grew during the 1959 inflation and eruption.

A high proportion (five out of seven) of the inclusions that formed at pressures >1.5 kbar were erupted in the hottest (Iki 22) magma. However, most of even the Iki 22 pressures are typical of the upper part of Kilauea's summit magma storage reservoir (Ryan, 1987b; Thurber, 1987). Even a kinked olivine has a low CO_2 inclusion, indicative of either low-pressure formation or reequilibration (Brown and Anderson, 1991). The one inclusion (22-8) that formed at about 5 kbar is in an unzoned, euhedral crystal.

Growth of millimeter-sized olivine crystals in a few days' time contrasts with conventional ideas of rates of crystallization. Mangan (1990) concluded, by applying crystal growth rates for plagioclase and ilmenite from the Makaopuhi lava lake (Cashman and Marsh, 1988) to crystal size data on olivine from the 1959 eruption, that the 1959 olivines resided in a storage reservoir for about 10 yr prior to the eruption. In our judgment, the variety of olivine textural types, inclusion compositions, and formation pressures indicate that the Kilauea Iki olivine crystals formed in a more complex system than a single, static boundary layer like the Makaopuhi lava lake.

If the time required for olivine aggregation is longer than a few months, then most inclusions and host crystals would be at least this old because almost all of the mass of olivine in the 1959 scoria is in aggregates (Schwindinger and Anderson, 1989). Helz (1987 and personal communication) questions whether olivine aggregation could occur rapidly because no further aggregation occurred in spite of olivine settling during 20 yr of lava lake cooling and solidification. Some aggregates contain inclusions that formed at significantly different pressures (45-A1 and 2) or from different melts (22-13-C1 and 2). Therefore, some aggregation occurred after low-pressure degassing and after magmatic evolution. In our judgment, the evidence offered by the melt inclusions and the zoning profiles of

the olivines (Schwindinger, 1987; Schwindinger and Anderson, 1989) provides a compelling basis for associating the zonation and aggregation of most of the 1959 olivine crystals with the months of inflation and eruption. Perhaps olivine supersaturation was too meager in the lava lake to cause olivines to grow together.

If the new magma were buoyant relative to the stored magma, then both magma mixing and low-pressure crystallization of olivine and formation of inclusions would follow naturally: the new magma would rise through and mix with stored magma, thereby cooling and crystallizing olivine.

Because magma density is sensitive to CO_2 gas, a picritic magma rich in olivine could be buoyant if it contained bubbles. We calculated bulk densities of parental and evolved magmas that would form by crystallization of Fo 87 olivine from melt with 15.0 wt% MgO and 0.2 wt% dissolved H_2O at temperatures given by T(°C) = 20.1(wt% MgO) + 1014 (Helz and Thornber, 1987). Melt and olivine densities were based on Lange and Carmichael (1987), and gas densities were calculated following Holloway (1977) and Flowers (1979). Although early 1959 magma contained an average of about 11 wt% of olivine phenocrysts [based on Murata and Richter's (1966) average early bulk magma and Helz's (1987) 10.0 wt% MgO in early melts], it would be buoyant relative to crystal- and gas-free stored melt with about 7 wt% MgO at pressures <1.0 kbar, if the 1959 magma contained at least 0.3 wt% of total CO_2. Such CO_2 contents are consistent both with gas monitoring studies (Greenland et al., 1985; Gerlach and Graeber, 1985) of other historic Kilauean eruptions and with deformation studies (Johnson, 1992). Anderson and Harris (unpublished data) show that the composition of scoria glass from November 18, 1959, is consistent with about 0.16 wt% CO_2 in a bulk magma with 20 wt% of olivine (equivalent to 0.22 wt% CO_2 in olivine-free magma).

Olivine crystallization and inclusion formation could be rapid because mixing would be turbulent (Huppert et al., 1986), in view of the viscosities (Ryan and Blevins, 1987) and densities (see above) of input parental and stored magmas and the magma supply rates at Kilauea (Dzurisin et al., 1984). That erupted material was both rich in gas-yielding high fountains (Wilson and Head, 1981) and rich in olivine suggests that the loss of both olivine and bubbles was minor, probably because storage time was short. Cooling and crystallization of olivine during mixing could be more rapid than cooling and crystallization beneath a thick lava lake crust, as assumed by Mangan (1990).

Eruption of picritic magma is unusual at Kilauea, as it is elsewhere. The circumstances that led to the atypical 1959 eruption probably include a seldom-used pathway that the new magma took toward the summit reservoir in 1959 (Helz, 1987), together with the youthful and probably segmented nature (Fiske and Kinoshita, 1969) of the summit reservoir (youthful because the reservoir that drained during the 1924 explosion, refilled since 1952). Consequently, the new magma was able to rise to a high level (i.e., low pressure), bypassing the deeper parts of the main reservoir, and intersect a body of stored magma at a shallow level. It was probably the unusually low pressure at which the new magma first encountered stored magma that led to the new magma's buoyancy.

We interpret the preponderance of low-pressure inclusions in Kilauean 1959 olivine crystals to signify that these formed as gassy, buoyant parental magma rose through and mixed with cooler, degassed magma in a near-summit reservoir that was shallow ($<\sim 1$ kbar).

Broader implications and speculations

The base of the summit magma storage reservoir may be controlled by the crushing strength of basalt and located at a pressure near 2 kbar (Ryan, 1987a, 1987b; Thurber, 1987; and see Johnson, 1992). At pressures >2 kbar crystal-free parental magma (14 wt% MgO) with up to 0.24 wt% total CO_2 content would be denser than residual melt (7 wt% MgO) free of both gas and crystals, because of the effect of pressure on both the solubility and density of CO_2 gas. About 0.2 wt% of CO_2 in parental basaltic magma may therefore be a critical concentration: if there is commonly less CO_2, then new parental magma may pond at depth.

Because near-summit eruptions of olivine-rich magma, like the 1959 magma, are rare, it seems reasonable to surmise that the usual behavior for Kilauea and most other shield volcanoes is for newly arriving parental magma to pond at the base of a summit magma storage reservoir. This level would be at the same pressure, but at different depths on different planetary bodies. Parental magmas with $>\sim 0.3$ wt% of CO_2 (certain alkali basalts on Earth?) would be buoyant at the reservoir base and would not pond there. Without ponding of magma at the reservoir base, a significant summit magma storage reservoir might not form. Without summit magma storage reservoirs, shield volcanoes marked by repeated summit eruptions, persistent summit degassing, and major subsurface migration of degassed magma might be replaced by decentralized fields of monogenetic vents. We therefore hypothesize that most shield volcanoes are fed by parental magmas that are so poor in volatiles that effervescence at about 2 kbar does not yield a buoyant product.

Acknowledgments

Kathleen Schwindinger, Christa Huey, Christine Skirius, and Mike Dolan helped prepare and analyze some of the inclusions reported here. Jacqueline E. Dixon helped guide us in reading and interpreting the FTIR spectra and also supplied analyses of four melt inclusions (22-1-10, 22-4G, 5-9, 5-12). We thank Thomas L. Wright of the Hawaiian Volcano Observatory for donating samples of the 1959 scoria for study. Discussions with Dave Harris and Kathy Schwindinger and reviews by Terry Gerlach and Rosalind T. Helz were especially helpful. Some of the computations involved in this work were clarified in a graduate course at Chicago (Amy Alberts, Xiangsheng Hu, Ping Liu, Aaron Pietruszka, and Matthew Slagel, students). We appreciate the support of NSF grant EAR 8915391.

References cited

Brown, G., and Anderson, A.T., Jr. (1991) Deformation in Kilauean olivine crystals. Geological Society of America Abstracts with Programs, 23, A450.

Cashman, K.V., and Marsh, B.D. (1988) Crystal size distributions (CSD) in rocks and the kinetics and dynamics of crystallization. II. Makaopuhi lava lake. Contributions to Mineralogy and Petrology, 99, 292–305.

Dixon, J.E., Stolper, E., and Delaney, J.R. (1988) Infrared spectroscopic measurements of CO_2 and H_2O in Juan de Fuca Ridge basaltic glasses. Earth and Planetary Science Letters, 90, 87–104.

Dixon, J.E., Clague, D.A., and Stolper, E.M. (1991) Degassing history of water, sulfur, and carbon in submarine lavas from Kilauea Volcano, Hawaii. Journal of Geology, 99, 371–394.

Dzurisin, D., Koyanagi, R.Y., and English, T.T. (1984) Magma supply and storage at Kilauea Volcano, Hawaii, 1956–1983. Journal of Volcanology and Geothermal Research, 21, 177–206.

Eaton, J.P. (1962) Crustal structure and volcanism in Hawaii. American Geophysical Union Monograph, 6, 13–29.

Eaton, J.P., and Murata, K.J. (1960) How volcanoes grow. Science, 132, 925–938.

Eaton, J.P., Richter, D.H., and Krivoy, H.L. (1987) Cycling of magma between the summit reservoir and Kilauea Iki lava lake during the 1959 eruption of Kilauea Volcano. U.S. Geological Survey Professional Paper, 1350, 1307–1335.

Fine, G., and Stolper, E. (1986) Carbon dioxide in basaltic glasses: Concentrations and speciation. Earth and Planetary Science Letters, 76, 263–278.

Fiske, R.S., and Kinoshita, W.T. (1969) Inflation of Kilauea Volcano prior to its 1967–1968 eruption. Science, 165, 341–349.

Flowers, G.C. (1979) Correction of Holloway's (1977) adaptation of the modified Redlich-Kwong equation of state for calculation of the fugacities of molecular species in supercritical fluids of geological interest. Contributions to Mineralogy and Petrology, 69, 315–318.

Gerlach, T.M., and Graeber, E.J. (1985) Volatile budget of Kilauea Volcano, Hawaii. Nature, 313, 273–277.

Greenland, L.P., Rose, W.I., and Stokes, J.B. (1985) An estimate of gas emissions and magmatic gas content from Kilauea Volcano. Geochimica et Cosmochimica Acta, 49, 125–129.

Hamilton, D.L., Burnham, C.W., and Osborn, E.F. (1964) The solubility of water and effects of oxygen fugacity and water content on crystallization in mafic magmas. Journal of Petrology, 5, 21–39.

Harris, D.M. (1982) H_2O, K_2O, P_2O_5, and Cl in basaltic glasses from Kilauea Volcano and Loihi Seamount, Hawaii (abs.). Eos, 63, 1138.

Harris, D.M., and Anderson, A.T., Jr. (1983) Concentrations, sources and losses of H_2O, CO_2 and S in Kilauean basalt. Geochimica et Cosmochimica Acta, 47, 1139–1150.

Helz, R.T. (1987) Diverse olivine types in lava of the 1959 eruption of Kilauea Volcano and their bearing on eruption dynamics. U.S. Geological Survey Professional Paper, 1350, 691–722.

Helz, R.T., and Thornber, C.R. (1987) Geothermometry of Kilauea Iki lava lake, Hawaii. Bulletin of Volcanology, 49, 651–668.

Holcomb, R., Moore, J., Lipman, P., and Bederson, R. (1988) Voluminous submarine lava flows from Hawaiian volcanos. Geology, 16, 400–404.

Holloway, J.R. (1977) Fugacity and activity of molecular species in supercritical fluids. In G.D. Fraser, Ed., Thermodynamics in geology, p. 161–181. Reidel, Dordrecht, The Netherlands.

Huppert, H.E., Sparks, R.S.J., Whitehead, J.A., and Hallworth, M.A. (1986) Replenishment of magma chambers by light inputs. Journal of Geophysical Research, 91, 6113–6222.

Johnson, D.J. (1992) Dynamics of magma storage in the summit reservoir of Kilauea Volcano, Hawaii. Journal of Geophysical Research, 97, 1807–1820.

Jurewicz, A.J.G., and Watson, E.B. (1988) Cations in olivine. II. Diffusion in olivine xenocrysts, with applications to petrology and mineral physics. Contributions to Mineralogy and Petrology, 99, 186–201.

Lange, R.A., and Carmichael, I.S.E. (1987) Densities of Na_2O-K_2O-CaO-MgO-FeO-Fe_2O_3-Al_2O_3-TiO_2-SiO_2 liquids: New measurements and derived partial molar properties. Geochimica et Cosmochimica Acta, 51, 2931–2946.

Mangan, M.T. (1990) Crystal size distribution systematics and the determination of magma storage times: The 1959 eruption of Kilauea Volcano, Hawaii. Journal of Volcanology and Geothermal Research, 44, 295–302.

Mathez, E.A., Blacic, J.D., Beery, J., Hollander, M., and Maggiore, C. (1987) Carbon in olivine: Results from nuclear reaction analysis. Journal of Geophysical Research, 92, 3500–3506.

Moore, J.G. (1965) Petrology of deep sea basalt near Hawaii. American Journal of Science, 263, 40–52.

Murata, K.J., and Richter, D.H. (1966) Chemistry of the lavas of the 1959–60 eruption of Kilauea Volcano, Hawaii. U.S. Geological Survey Professional Paper, 537-A, 26 p.

Newman, S., Stolper, E.M., and Epstein, S. (1986) Measurement of water in rhyolitic glasses: Calibration of an infrared spectroscopic technique. American Mineralogist, 71, 1527–1541.

Qin, Z., Lu, F., and Anderson, A.T., Jr. (1992) Diffusive reequilibration of melt and fluid inclusions. American Mineralogist, 77, 565–576.

Richter, D.H., Eaton, J.P., Murata, K.J., Ault, W.U., and Krivoy, H.L. (1970) Chronological narrative of the 1959–60 eruption of Kilauea Volcano, Hawaii. U.S. Geological Survey Professional Paper, 537-E, 73 p.

Roedder, E. (1965) Liquid CO_2 inclusions in olivine-bearing nodules and phenocrysts from basalts. American Mineralogist, 50, 1746–1782.

Ryan, M.P. (1987a) Neutral buoyancy and the mechanical evolution of magmatic systems. In B.O. Mysen, Ed., Magmatic processes: Physicochemical principles, Special Publication number 1, p. 259–287. Geochemical Society, College Park, Pennsylvania.

——— (1987b) Elasticity and contractancy of Hawaiian olivine tholeiite and its role in the stability and structural evolution of subcaldera magma reservoirs and rift systems. U.S. Geological Survey Professional Paper, 1350, 1395–1447.

Ryan, M.P., and Blevins, J.Y.K. (1987) The viscosity of synthetic and natural silicate melts and glasses at high temperatures and 1 bar (10^5 Pascals) pressure and at higher pressures. U.S. Geological Survey Bulletin, 1764, 563 p.

Schwindinger, K.R. (1987) Petrogenesis of olivine aggregates from the 1959 eruption of Kilauea Iki: Synneusis and magma mixing, 213 p. Ph.D. thesis, University of Chicago, Chicago, Illinois.

Schwindinger, K.R., and Anderson, A.T., Jr. (1989) Synneusis of olivine and crystal settling beneath Kilauea. Contributions to Mineralogy and Petrology, 103, 187–198.

Stolper, E. (1982) Water in silicate glasses: An infrared spectroscopic study. Contributions to Mineralogy and Petrology, 81, 1–17.

Stolper, E.M., and Holloway, J.R. (1988) Experimental determination of the solubility of carbon dioxide in molten basalt at low pressure. Earth and Planetary Science Letters, 87, 397–408.

Tait, S. (1992) Selective preservation of melt inclusions in igneous phenocrysts. American Mineralogist, 77, 146–155.

Thurber, C.H. (1987) Seismic detection of the summit magma complex of Kilauea Volcano, Hawaii. Science, 223, 165–167.

Watson, E.B., Sneeringer, M.A., and Ross, A. (1982) Diffusion of dissolved carbonate in magmas: Experimental results and applications. Earth and Planetary Science Letters, 61, 346–358.

Wilson, L., and Head, J.W., III (1981) Ascent and eruption of basaltic magma on the earth and moon. Journal of Geophysical Research, 86, 2971–3001.

Wright, T.L. (1973) Magma mixing as illustrated by the 1959 eruption of Kilauea Volcano, Hawaii. Geological Society of America Bulletin, 84, 849–858.

Wright, T.L., and Fiske, R.S. (1971) Origin of the differentiated and hybrid lavas of Kilauea Volcano, Hawaii. Journal of Petrology, 12, 1–65.

Wright, T.L., Swanson, D.A., and Duffield, W.A. (1975) Chemical composition of Kilauea east-rift lava, 1968–1971. Journal of Petrology, 16, 110–133.

Manuscript received June 8, 1992
Manuscript accepted March 5, 1993